ΔNp63γ/SRC/Slug signalling axis promotes epithelial-to-mesenchymal transition in squamous cancers

ΔNp63γ/SRC/Slug signalling axis promotes epithelial-to-mesenchymal transition in squamous cancers

Kirtiman Srivastava[1+], Adam Pickard[1,2], Stephanie G Craig[1], Gerard P Quinn[1], Shauna M Lambe[1], Jacqueline A James[1], Simon S McDade[1*+], Dennis J. McCance[3*+]

[1]Centre for Cancer Research and Cell Biology, Queen's University Belfast, Belfast, BT9 7AE, UK

[2]The Welcome Trust Centre for Cell Matrix Research, University of Manchester, Manchester, M13 9PL, UK

[3]Department of Pathology, School of Medicine, University of New Mexico, Albuquerque, NM 87131-0001, USA

*These authors contributed equally to this work

+ Corresponding authors:

Prof. Dennis J. McCance

Department of Pathology

School of Medicine

University of New Mexico

Albuquerque, NM 87131-0001

USA

Tel: 505-272-0624

E-mail: dmccance@salud.unm.edu

Dr. Simon McDade

Centre for Cancer Research and Cell Biology,

Queen's University Belfast

97 Lisburn Road, Belfast BT9 7AE

UK

Tel: 0044 2890972183

E-mail: s.mcdade@qub.ac.uk

Dr. Kirtiman Srivastava

Centre for Cancer Research and Cell Biology,

Queen's University Belfast

97 Lisburn Road, Belfast BT9 7AE

UK

Tel: 0044 2890972803

E-mail: k.srivastava@qub.ac.uk

Running title: p63/SRC/Slug axis modulates EMT and invasion

Conflict of interest

The authors declare no potential conflicts of interest.

Source of funding

Medical Research Council (MRC), UK grant G1001692

Translational relevance

We used TCGA datasets from Head and Neck Squamous Cell Carcinoma (HNSCC) patients and patient-derived tumour sections from Human Papilloma Virus (HPV)-positive/-negative oropharyngeal HNSCC to clinically validate *in vitro* data generated using primary human foreskin keratinocytes (HFK) expressing the HPV16 E6/E7 oncogenes. The novel and translational aspects of this study are;

1. Slug/SNAI2 is the main epithelial-to-mesenchymal transition (EMT)-activating transcription factor in HNSCC and E6/E7-HFK,
2. Activation of SRC and downstream targets mediate the Slug/SNAI2-evoked EMT,
3. We show for the first time that a particular p63 isoform, namely, ΔNp63γ is necessary and sufficient to activate SRC signalling axis, induce EMT and invasion.

This manuscript is relevant to those investigating **(a)** the oncogenic significance of p63 transcription factors, **(b)** the role of upstream pathways in the activation of Slug, and **(c)** the therapeutic potential of SRC inhibitors in clinical trials on epidermal growth factor receptor resistant HNSCC patients.

Abstract

Purpose: To investigate the regulation of epithelial-to-mesenchymal transition (EMT) in Head and Neck Squamous Cell Carcinoma (HNSCC) and its importance in tumour invasion.

Experimental design:

We use a 3D invasive organotypic raft culture model of human foreskin keratinocytes expressing the E6/E7 genes of the Human Papilloma Virus-16, coupled with bioinformatic and immunhistochemical analysis of patient samples to investigate the the role played by EMT in invasion and identify effectors and upstream regulatory pathways.

Results: We identify SNAI2 (Slug) as a critical effector of EMT activated downstream of TP63 overexpression in Head and Neck Squamous Cell Carcinoma (HNSCC). Splice-form specific depletion and rescue experiments further identify the ΔNp63γ isoform as both necessary and sufficient to activate the SRC signalling axis and SNAI2-mediated EMT and invasion. Moreover, elevated SRC levels are associated with poor outcome in HNSCC patients in the cancer genome atlas dataset. Importantly, the effects on EMT and invasions and SNAI2 expression can be reversed by genetic or pharmacological inhibition of SRC.

Conclusion: Overexpression of ΔNp63γ modulates cell invasion by inducing targetable SRC-Slug-evoked EMT in HNSCC, which can be reversed by inhibitors of the SRC signalling.

Key words: Human papilloma virus (HPV), keratinocytes, p63, Src, Slug, epithelial-to-mesenchymal transition (EMT)

Introduction

Head and Neck Squamous Cell Carcinoma **(**HNSCC) represents the sixth most commonly diagnosed cancer worldwide (>500,000 new cases pa) (1). The frequency of HNSCC is increasing, particularly in a younger age group associated with HPV infection, which accounts for 23-60% of cases (2). Currently there are limited options for biomarker-guided, molecular-targeted therapies in HNSCC because of a poor understanding of the disease at the molecular level.

Amplification and overexpression of TP63 occurs independently of TP53 mutation or HPV infection in the majority of SCCs (3,4), the clinical importance of which remains unclear. The TP63 locus is complex and encodes at least six well-described isoforms that play overlapping but distinct roles in activating or repressing target gene expression. This occurs as a result of utilisation of two alternative promotors resulting in TA (transactivation) and ΔN (lacks the TA domain) N-terminal isoforms, each of which can be alternatively spliced with C-terminal variants α, β and γ (5). Traditionally, elevated expression of the predominant ΔNp63α isoform has been assumed to promote SCC growth by opposing activation of canonical TP53/TP73 regulated cell cycle repressive and pro-apoptotic targets (6,7). Importantly, recent data from our group and others indicate that TP63 plays essential TP53-independent roles in promoting and maintaining squamous transformation stimulating invasion and migration and is paradoxically, necessary to induce differentiation in normal cells (8-10). Our integrative genome-wide analyses of TP53-TP63 function highlighted the extent of the network of genes potentially affected by the TP63-TP53 axis, and the importance of up-regulation of TP63 target genes in HNSCC (11,12).

Previously, we and others have shown that TP63 is involved in supporting an Epithelial-to-Mesenchymal Transition (EMT)-phenotype in normal breast epithelial

cells (13,14). E-cadherin (CDH1), an adherens junction protein and an epithelial marker, is essential for knitting the epithelial cells together, and the loss (through suppression of CDH1 expression and/or its relocalisation away from cell-cell contacts) is critical for the acquisition of EMT (15). This can be mediated through the activities of EMT-inducing transcription factors including Twist (TWIST1), Snail (SNAI1) and Slug (SNAI2), which are known to directly repress transcription from the CDH1 promoter thereby promoting the disassembly of the cell-cell contacts (16,17). Vimentin, a hallmark of EMT encoded by the VIM gene, is also overexpressed in malignant epithelial breast and vulvar cancers and correlates with poor prognosis (18,19). Hence in invasive cancers, several molecular pathways are altered to support the upregulation and protein stabilisation of EMT-promoting genes.

We recently used a 3D-organotypic model of human foreskin keratinocytes (HFK) stably expressing the high-risk HPV-16 E6 and E7 oncoproteins (E6/E7-HFK) to identify the non-receptor tyrosine kinase Src, as a TP63 target gene in oro-pharyngeal cell carcinoma, a subset of HNSCC (8,20,21). Src is a critical regulator of cell migration, the upregulation of which has been observed in several cancers including HNSCC, where this has a direct correlation with disease progression (18,19). Our study elucidated the importance of TP63 in transcriptionally regulating a Src-MMP axis that is required for migration and invasion, which could be inhibited by TP63 or Src depletion or Src activity inhibition.

In this study, we show for the first time that the ΔNp63γ isoform is an important factor in regulating EMT through Slug/SNAI2 and SRC and that the EMT phenotype and invasion can be reversed by inhibition of SRC activity.

Material and methods

Cell culture

Primary neonatal HFK expressing an empty vector (pBabe-HFK) or E6/E7-HFK were cultured as monolayer to subconfluence in Epilife medium on collagen-I coated plates before harvesting mRNA and proteins. A fraction of these cells were seeded on Rb-depleted human foreskin fibroblast embedded in collagen-I plugs to establish 3D-organotypic rafts for studying invasion (8,22). After 14 days of incubation in E-medium, the rafts were sliced, embedded in paraffin, sectioned and used for immunofluorescence and H&E stains. The invasive incidents were quantified using H&E stained sections and represented as number of invasions/cm recorded from three independent experiments.

Retroviral constructs and stable knockdown

The stable knockdowns of non-specific (scram) or p63 isoforms (UTR, DBD) in E6/E7-HFK were established by shRNA molecules (9) ligated in the pSuper-retro-neo constructs before their transfection in the 293T cells. The retroviruses generated using the phoenix system were used to infect HFK and GFP-tagged constructs acted as positive controls for measuring infection efficiency (22).

Adenovirus-mediated overexpression

To generate shRNA resistance ΔNp63α/β/γ isoforms, 5µg of entry vector pENTR11(Life technologies) carrying the gene of interest (GFP or ΔNp63α/β/γ) were subjected to site directed mutagenesis for four point mutations as previously described (13), and were sequence verified before recombination with the adenoviral pAd/CMV/V5-DEST Gateway vector (Life technologies, UK) using Gateway-LR Clonase-II enzyme mix (Life technologies) according to the manufacturer's

guidelines. Similarly, the constitutively active Src (Src-531) construct was generated by site-directed mutagenesis (8) before recombination with adenoviral vector. The recombined vector was transfected in 293T cells before generation, purification and titration of adenovirus as previously described (23).

Transient knockdown

Transient gene/protein knockdowns in E6/E7-HFK were established by transfection with 50 nM of non-specific (scram) or specific siRNA molecules targeting Slug (mol-1:5'-CAAACGACTTTGCAACTCC-3', mol-2:5'-CCTCTTGGCATACTCCTCT-3') (24), Src and p63 (UTR, Pan) as previously described (8).

RNA extraction and quantitative real-time polymerase chain reaction (RT-PCR)

The total RNA was harvested from HFK samples using Trizol reagent (Roche, USA) according to the manufacturer's instructions. After measuring the purity, 1µg RNA was used to synthesise cDNA by single-strand cDNA synthesis kit (Roche, USA) followed by PCR amplification to study the fold difference in mRNA levels after normalisation against reference gene RPLP0 as previously described (12).

Western blotting

50µg of whole cell lysates were resolved on 10% SDS-PAGE gels before transfer of proteins onto nitrocellulose membrane which was followed by blocking in 5% milk and incubation with primary antibodies against human E-cadherin, N-cadherin, Fibronectin (BD biosciences), Slug, Snail, vimentin, Src, Src-pY^{416}, AKT-pS^{473}, AKT (Cell signalling), p63 (Abcam), Twist, ZEB1, ZEB2 (Santa Cruz Biotech) GAPDH and β-actin (Sigma-Aldrich). Using HRP-tagged species specific-secondary antibodies, the differential protein expressions were visualised by chemiluminescence detection.

Immunofluorescence

The cellular localisation of proteins was studied by fixing monolayer of HFK, which was followed by permeabilisation and exposure to primary and species-specific Alexa-fluor-488/594-tagged secondary antibodies (Life technologies). The proteins were visualised through 20x and 60x magnification by confocal microscopy. The cellular localisation of proteins in HNSCC sections or on 3D-organotypic rafts were studied by heat induced antigen retrieval methods (tris buffer and citrate buffer) followed by immunofluorescence detection. The intensities of staining (Q-score) were quantified as previous described (8).

TCGA dataset analysis

HNSCC samples processed for the TCGA resource (4) were utilised for *in silico* analyses/support of laboratory findings. Processed (level three) gene expression data for 277 HNSCC patients, 277 tumour and 44 matched normal tissue, was downloaded from Gene Expression Omnibus, GEO ascension number GSE62944 (25) and supporting clinical data from University of California Santa Cruz Cancer Browser (https://genome-cancer.ucsc.edu/proj/site/hgHeatmap/). HPV Status was previously defined by the TCGA (5) in these samples, as the presence of >1000 mapped RNA sequencing reads aligning to HPV viral genes E6 and E7 (5) and was obtained through cbioportal (http://www.cbioportal.org/). Gene expression data was log2(x+1) transformed before merging with clinical data. The resulting data matrix was used to plot expression of genes of interest between normal, HPV positive and negative. Patients were dichotomised into high/low expressing groups for survival analyses by receiver-operating characteristic analysis of the gene of interest against survival as previously described (26). Survival analyses were performed using the Kaplan-Meier estimate on a sub-cohort of 241 HPV negative patients with survival data and the log-

rank test used to calculate univariate associations between genes of interest and survival. Only five year survival was considered and defined as the time, in months, from sample collection until death by any cause, with right censoring applied to patients lost to follow-up or with a survival time of greater than 60 months. These analyses were performed using R v.3.3.1.

ChIP-seq and analysis of Public ChIP-seq datasets

TP63 ChIP-seq data was generated from HFK-E6E7 expressing cells as previously described (12). Raw FASTQ data and those from our previously published ChIP-seq for p63 in primary HFKs (12) were re-analysed as follows: Adapter sequences were removed and FASTQC conducted with trimgalore and resulting reads aligned to hg19 with Bowtie 2 default settings (27). Reads filtered for blacklist regions with samtools were used as inputs for peak calling with MACS2 (28) comparing ChIP with input control and resultant SPMR normalised bedgraphs converted to bigwig format for visualisation using UCSC bedGraphToBigWig script. Relevant bigwig files from encode (29) were downloaded and visualised alongside p63. Integrative analysis of narrowpeak calls was conducted using custom workflows in Cistrome (30).

Statistics

The statistics for lab experiments were performed by comparing the mean values by student's *t*-test and one-way analysis of variance (ANOVA) followed by Dunnet's post hoc analysis using IBM SPSS 20.0 software. The results were presented as mean±s.e.m. from five independent experiments and $P<0.05$ was considered to be significant in all the experiments. For TCGA gene expression analysis, results were presented as mean±s.e.m. and statistical significance defined as $^{***}P<0.001$, $^{**}P<0.01$, and $^{*}P<0.05$ when calculated by either Welch's t-test (A) or ANOVA (C, D) when compared to the normal/controls.

Results

Slug/SNAI2 is the predominant EMT-promoting gene expressed in HNSCC

To investigate de-regulation of EMT-promoting transcription factors in HNSCC, we first examined expression of EMT master regulatory transcription factors Twist/TWIST1, Snail/SNAI1 and Slug/SNAI2, in HNSCC patient samples in The Cancer Genome Atlas (TCGA) (HPV positive (n=36) and HPV negative (n=241) (4). This revealed that expression of SNAI1, SNAI2 and TWIST1 were significantly increased in both HPV positive and negative tumours compared to normal (Figure 1A). Importantly, while signficant increases of both SNAI1 and TWIST1 were observed, the absolute expression levels of SNAI1/Snail and TWIST1 were 5-10 fold lower than Slug/SNAI2 as measured by FPKM (fragments per kilobase of exon per million fragments mapped) (Figure 1A), with SNAI1 and TWIST exhibiting more modest fold change in expression compared to normal than SNAI2/Slug (SNAI2 2.02/3.70; SNAI1 1.40/1.59, TWIST1 1.51/1.89 in HPV+ve and HPV-ve tumours respectively) suggesting that Slug/SNAI2 is the predominantly expressed EMT-regulating transcription factor activated in HNSCC. Further examination of expression levels and correlation of SNAI1, SNAI2, TWIST1 and other EMT regulators ZEB1 and ZEB2 and markers Vimentin (VIM), E-Cadherin (CDH1), N-Cadherin (CDH2) and Fibronectin (FN1); revealed similarly modest expression of both ZEB1 and ZEB2, with only ZEB2 demonstrating significant upregulation (ZEB1 1.09/1.16; ZEB2 1.36/1.33 in HPV+ve and HPV-ve tumours respectively.

In support of the prediction that Slug/SNAI2 is important for EMT, we observed significant increases in Slug/SNAI2 protein levels (as measured by indirect immunfluorescent staining) when comparing tumour versus adjacent normal in full face sections of both HPV positive (n=5), and HPV negative (n=6) oropharyngeal

HNSCC (Figure 1B and C and Supplementary Figure S2A). Interestingly, in agreement with recent studies in normal skin (31), only a few basal cells in normal regions stained positive for Slug/SNAI2,whereas, in contrast, intense nuclear localisation of Slug/SNAI2 was observed throughout both HPV positive and negative tumours (Figure 1B and C and Supplementary Figure S2A). In addition, the faint staining of Snail/SNAI1 and TWIST1 proteins in epithelial cells from normal and tumour sections suggested low protein expression in these cells compared to the adjacent stromal cells (Supplementary Figure S2A).

Further evaluation of SNAI1, SNAI2, TWIST1, ZEB1 and ZEB2 protein and mRNA levels in our invasive HPV-E6/E7 expression model system (8,22,32), also indicates that Slug/SNAI2 is the predominant EMT-activating transcription factor expressed in E6/E7-HFK and normal matched keratinocyte controls, and is significantly up-regulated at both the mRNA and protein level in E6/E7-HFK (Figure 1D and E and Supplementary Figure S2B). Similar to TCGA patient analysis, while relative increases in both Twist/TWIST1 and Snail/SNAI1 mRNA expressions in E6/E7-HFK were also observed (Figure 1D), their levels were at the limit of detection by both RT-PCR and Western blot analysis (Figure 1D and Supplementary Figure S2B). Importantly, elevated Slug/SNAI2 coincided with a switch to spindle like morphology (Figure 1F), significant decrease in expression of both E-cadherin/CDH1 mRNA and protein and concomitant increase in Vimentin/VIM and Fibronectin/FN1 (Figure 1D, E and Supplementary Figure S2B) as well a loss of junctional E-Cadherin staining (Figure 1G); suggesting that E6/E7 expressing cells exhibit an EMT phenotpye.

Depletion of Slug attenuates EMT and mitigates invasion

To determine the functional contribution of Slug/SNAI2 in mediating EMT and invasion we used two independent siRNA molecules (24) to knockdown Slug/SNAI2 expression in E6/E7-HFK (Figure 2A-C and Supplementary S3A). Depletion of Slug/SNAI2 resulted in a reversal of EMT as measured by increase in mRNA and protein expression of E-cadherin, concomitant reduction in the expression of vimentin (Figure 2A and C), reversion of spindle-like to cobble-stone morphology and concurrent increase in E-cadherin/CDH1 localisation at cell junctions (Figure 2C and Supplementary Figure S3A). Importantly, qualitative and quantitative analysis of 3D-organotypic rafts established using E6/E7-HFK with confirmed knockdown of Slug expression by the more effective siRNA (mol-2) showed a significant reduction in number of invasions (Figure 2D and E) and that these effects were independent of cell proliferation as measured by BrdU uptake (Supplementary Figure S3B and C), indicating that Slug/SNAI2 is necessary for both EMT and invasion in this model.

SRC signalling axis modulates the expression of EMT markers

Western blot analysis revealed that Slug/SNAI2 depletion (Supplementary Figure S4A) did not affect SRC levels and activatory phosphorylation (Y^{416}), which we have previously shown to be necessary and sufficient for invasion. We next evaluated whether Slug/SNAI2 was activated downstream of SRC and required for EMT and invasion. In support of this hypothesis both Slug/SNAI2 mRNA and protein expression were significantly decreased in 2D-culture upon transient siRNA mediated depletion of SRC expression with two independent siRNAs (Figure 3A and B). Moreover, a similar reduction of Slug/SNAI2 protein was observed upon inhibition of Src activity using the kinase inhibitor dasatanib, both in 2D-culture (Figure 3C)

and in treated organotypic raft cultures (Figure 3D), where we previously demonstrated the ability of dasatanib or SRC depletion to block invasion (8). In support of a mechanistic role for EMT, both SRC depletion or inhibition were accompanied by a cognate decreased vimentin and increased E-cadherin expression (Figure 3A-C) and restoration of gross cellular morphology suggestive of a reversion of EMT (Supplementary Figure S4B). Moreover, exogenous adenoviral expression of constitutively active Src (Src-531), which is sufficient to promote cell invasion (8), also upregulated the protein expression of Slug and vimentin, while suppressing E-cadherin and inducing EMT morphology in non-invasive cells (Supplementary Figure S4C, D).

Analysis of TCGA patient RNA-seq data revealed that SRC mRNA expression is significantly elevated in both HPV positive and negative HNSCC tumours compared to normal (Figure 3E). Importantly, dichotomising patients into high and low expressing groups (based on receiver operator curve (ROC) outcome based dichomisation of 5-year overall survival) (26), identified a significant association between high SRC expression (high=48, low=192) and worse outcome in HPV negative patients (Figure 3F).

Ascertaining impact of intratumoural expression of other EMT transcription factors (SNAI1/Snail, TWIST1, ZEB1 and ZEB2) and markers (CDH1, CDH2, VIM, FN1) on survival is challenging owing to the high level expression of EMT factors in stromal cells (Figure 1 B and Supplementary Figure S2 A). Further analysis revealed high levels of correlation between all of these stromally derived markers (data not shown) and no coherent pattern of impact on outcome (Data not shown).

TP63 modulates the expression of SNAI2

Interestingly, a similar trend was observed for total TP63 expression (Figure 4A), where high TP63 levels were associated with worse outcome. Since we have previously shown that TP63 is necessary to effect invasion in this model by regulating SRC-AKT-AP1 signalling (8), we next compared TP63-ChIP-seq in E6/E7-HFK with our previous TP63 ChIP-seq in primary HFKs (12) (Supplementary Figure S5A). Similar TP63 binding patterns were observed globally and specifically at the previously described *SRC* (Figure 4B) and *MMP14* (not shown) associated enhancer regions (8). Furthermore, we also identified direct TP63 binding to upstream enhancer and promoter of *SNAI2* and upstream and within *CDH1* loci (E-cadherin) (Figure 4B and Supplementary Figure S5B). Importantly, siRNA mediated depletion of all TP63 isoforms resulted in significant decreased Slug/SNAI2 mRNA and protein levels (Figure 4C and D). Significantly, depletion of Slug did not affect TP63 mRNA or mRNA splice-form or protein isoform expression (Supplementary Figure S6A and B) indicting that TP63 is required for SRC dependent transcription of Slug/SNAI2 and EMT that is necessary for invasion.

TP63γ isoform is necessary for the Src-Slug signalling, EMT and invasion

Since we and others have consistently observed differential and often opposing effects of expressing different TP63 isoforms on target gene expression and resulting phenotypes (11,33-35), we speculated that TP63 mediated activation of SRC and Slug/SNAI2 may be differentially affected by TP63 isoforms similar to our previous observations with regard to the role of ΔNp63γ isoform in affecting EMT in breast epithelial cells (13). To investigate this possibility, we first compared the effects of specifically depleting the α and β isoforms through targettiing their shared

3'UTR (UTR) (with a validated shRNA molecule that does not affect γ-isoforms) (9) with an shRNA targeting the DNA binding domain (DBD) and therefore depleting all TP63 isoforms (DBD); which we had previously reported to attenuate invasion in this model (8). This analysis revealed that depletion of the α and β isoforms had little or no effect on number of invasions (Supplementary Figure S7A-C) suggesting that residual γ-isoforms are sufficient to maintain invasive capacity. These results were further supported by similar analysis with independent siRNAs, where total p63 depletion (Pan molecule) was sufficient to significantly reduce the number of invasions (Figure 5A and B). In support of these results, mRNA or protein expression of Src, Slug/SNAI2, vimentin and Src activity were unaffected in UTR depleted cells grown in 2D on collagen I (Figure 5C-E), whereas in contrast, total TP63 knockdown depleted mRNA and protein expression of both Src and Slug (Figure 5D and E) with a concomitant increase in the protein levels of E-cadherin while suppressing vimentin (Figure 5D and E). Cumulatively, this suggests that the residual endogenous TP63γ isoform sufficient to maintain the expression/activity of Src-Slug signalling axis, EMT and and invasive phenotype.

ΔNp63γ is sufficient to induce Src-Slug axis, EMT and invasion

We have previously shown that ΔN N-terminal variants are the dominant forms in both normal (9) and E6/E7 expressing HFKs (36) with endogenous TA isoforms below the limit of Western blotting and not normally detectable by RT-PCR (data not shown). Therefore, we next tested if expression of ΔNp63γ or indeed ΔNp63α or ΔNp63β alone, is sufficient to rescue EMT and invasion in E6/E7-HFK rendered non-invasive through stable shRNA depletion of total TP63. To achieve this we compared the effects of adenoviral-mediated reintroduction of individual TP63 isoforms

rendered resistant to the shRNA into E6/E7-HFK cells (13). Growth of these reconstituted cells in organotypic cultures revealed that only re-expression of the ΔNp63γ isoform was capable of significantly inducing invasions (Figure 6A and B), whereas ΔNp63α had a modest repressive effect on residual invasion and ΔNp63β no significant impact. Importantly, ectopic expression of ΔNp63γ isoform in keratinocytes was sufficient to significantly upregulate mRNA levels of SRC and SNAI2, while suppressing CDH1 (E-cadherin) compared to its controls (GFP) (Figure 6C), co-incident with upregulation of protein expression of Src, activated Src, Slug, activated AKT and vimentin and suppression of E-cadherin (Figure 6D and Supplementary Figure S7D). Together these results identify a potentially important novel oncogenic role of ΔNp63γ isoform in E6/E7-HFK, which is sufficient to induced Src activated EMT and invasion in squamous cells.

Discussion

Depletion of cellular epithelial markers with concurrent appearance of those of mesenchymal cells is an important switch required to enable morphological and mechanical changes necessary to underpin the invasive capacity of cancer cells. Here, we identify that expression of ΔNp63γ isoform as both necessary and sufficient to induce such a switch in E6/E7 transformed primary human keratinocytes to promote an EMT-like phenotype and invasion. This is mediated through direct transcriptional modulation and activation of Slug/SNAI2 and Src, the increased expression of which is observed along with TP63 in both HPV positive and negative HNSCC patients. In particular, increased SRC levels correlates with poor prognosis and represents a

potential clinically actionable event through inhibition of Src or downstream AKT activity.

Our previous studies demonstrated that E6/E7-HFK exhibited increased cell migration and invasion compared to normal HFK (8). In this study we focused on determining the importance of master transcriptional regulators of EMT namely SNAI1/Snail, SNAI2/Slug, TWIST1/Twist, given their importance for EMT required for cancer cell migration, invasion and ultimately metastasis. Our analyses revealed that Slug is the dominant EMT regulator increased in both our invasive E6/E7-HFK model and in patient samples, wherein both Snail and Twist are expressed at much lower levels a finding that is strongly supported by a recent landmark single cell study of HNSCC patient samples (37) which indicates that the majority of signal for EMT markers with the exception of SNAI2/Slug are stromally derived in HNSCC and is associated with a partial EMT. Importantly, depletion of Slug is sufficient to reverse the increases in vimentin, decrease E-Cadherin, and change cells from a fibroblast-like to an epithelial-like morphology and prevent invasion in 3D organotypic cultures, suggesting Slug is necessary for the invasive phenotype. There is significant evidence in the literature to support the broader applicability of our findings with regard to the importance of SNAI2/Slug for HNSCC cell survival, migration, invasion, stemness and radioresistance (38-41). Consistent with our hypothesis, the overexpression of Slug/SNAI2 and its increased transcriptional activity in normal human keratinocytes has been shown to induce a) transcriptional silencing of differentiation genes, b) dedifferentiation, c) EMT, d) wound healing and e) enhanced cell migration (31,42,43).

Moreover, our IHC studies in HPV +ve and -ve oropharyngeal HNSCC are supported by findings by Wang et al., which indicated that elevated Slug/SNAI2

expression in HNSCC tumour cells in a cohort of 129 HNSCC correlated with poor prognosis (38). Since the expression or activities of components from TP63/Src signalling axis, remained unaffected by Slug/SNAI2 depletion it suggests that it is a downstream target of this signalling cascade. This is consistent with a recently published study which also identified Slug/SNAI2 as a direct p63 target in lung SCC and breast cancer cell lines (44).

Transcriptional and protein levels of TP63 isoforms are elevated in E6/E7-HFK and depletion of total TP63 isoforms has been previously shown to attenuate the cell invasion (8). However, in the current study stable knockdown of the TP63 α and β isoforms (UTR) in the invasive population had no significant impact in reducing the number of invasions. However, since total TP63 ablation depleted the expression of Src and reversed expression of EMT genes, it indicates that either TAp63γ or ΔNp63γ isoforms are responsible for promoting EMT and invasion. Our previous studies on normal breast cells have shown the role ΔNp63γ in promoting EMT phenotype and development of epithelial cancers (13). Since the ΔNp63 isoforms are more stable compared to the TAp63 isoforms due to the absence of structural features like the FWL motif which accelerates the TAp63 protein degradation (45,46), and since TAp63 levels are almost undetectable in HFK, we expressed ΔNp63 isoforms (α, β and γ) in a background where all TP63 isoforms were depleted by stable knockdown. Ectopic expression of the ΔNp63γ isoform only, induced invasion concomitant with activation of both SRC/AKT signalling and Slug-mediated EMT .

In conclusion, the ΔNp63γ isoform appears to be essential for mediating invasion by modulating the expression of Slug and by activating Src signalling. Specific inhibition of Src activity has a therapeutic potential alone or as recently suggested in combination with epidermal growth factor receptor and other receptor tyrosine kinase

inhibitors to protect against progression and relapse of HNSCC, which are problems in treating these cancers (47-49).

Acknowledgement

The authors thank Medical Research Council, UK grant G1001692 for funding this study. The patient samples used in this research were received from the Northern Ireland Biobank (NIB13-001) which has received funds from HSC Research and Development Division of the Public Health Agency in Northern Ireland and the Friends of the Cancer Centre. ChIP-seq data generation in this study was supported by the FMHLS, Genomics Core Technology Unit, Queen's University Belfast.

Supplementary information accompanies the paper on the CCR website

References

1. Ferlay J, Shin H-R, Bray F, Forman D, Mathers C, Parkin DM. Estimates of worldwide burden of cancer in 2008: GLOBOCAN 2008. International Journal of Cancer **2010**;127(12):2893-917 doi 10.1002/ijc.25516.
2. Goon PKC, Stanley MA, Ebmeyer J, Steinstraesser L, Upile T, Jerjes W, *et al.* HPV & head and neck cancer: a descriptive update. Head & Neck Oncology **2009**;1 doi 10.1186/1758-3284-1-36.
3. Hoadley KA, Yau C, Wolf DM, Cherniack AD, Tamborero D, Ng S, *et al.* Multiplatform Analysis of 12 Cancer Types Reveals Molecular Classification within and across Tissues of Origin. Cell **2014**;158(4):929-44 doi 10.1016/j.cell.2014.06.049.
4. Lawrence MS, Sougnez C, Lichtenstein L, Cibulskisl K, Lander E, Gabriel SB, *et al.* Comprehensive genomic characterization of head and neck squamous cell carcinomas. Nature **2015**;517(7536):576-82 doi 10.1038/nature14129.
5. Trink B, Okami K, Wu L, Sriuranpong V, Jen J, Sidransky D. A new human p53 homologue. Nature Medicine **1998**;4(7):747-8 doi 10.1038/nm0798-747.
6. McDade SS, McCance DJ. The role of p63 in epidermal morphogenesis and neoplasia. Biochemical Society Transactions **2010**;38:223-8 doi 10.1042/bst0380223.
7. Rocco JW, Leong CO, Kuperwasser N, DeYoung MP, Ellisen LW. p63 mediates survival in squamous cell carcinoma by suppression of p73-dependent apoptosis. Cancer Cell **2006**;9(1):45-56 doi 10.1016/j.ccr.2005.12.013.
8. Srivastava K, Pickard A, McDade S, McCance DJ. p63 drives invasion in keratinocytes expressing HPV16 E6/E7 genes through regulation of Src-FAK signalling. Oncotarget **2015**;Epub, DOI:10.18632.
9. McDade SS, Patel D, McCance DJ. p63 maintains keratinocyte proliferative capacity through regulation of Skp2-p130 levels. Journal of Cell Science **2011**;124(10):1635-43 doi 10.1242/jcs.084723.
10. Ramsey MR, Wilson C, Ory B, Rothenberg SM, Faquin W, Mills AA, *et al.* FGFR2 signaling underlies p63 oncogenic function in squamous cell carcinoma. Journal of Clinical Investigation **2013**;123(8):3525-38 doi 10.1172/jci68899.
11. McDade SS, Henry AE, Pivato GP, Kozarewa I, Mitsopoulos C, Fenwick K, *et al.* Genome-wide analysis of p63 binding sites identifies AP-2 factors as co-regulators of epidermal differentiation. Nucleic Acids Research **2012**;40(15):7190-206 doi 10.1093/nar/gks389.
12. McDade SS, Patel D, Moran M, Campbell J, Fenwick K, Kozarewa I, *et al.* Genome-wide characterization reveals complex interplay between TP53 and TP63 in response to genotoxic stress. Nucleic Acids Research **2014**;42(10):6270-85 doi 10.1093/nar/gku299.
13. Lindsay J, McDade SS, Pickard A, McCloskey KD, McCance DJ. Role of Delta Np63 gamma in Epithelial to Mesenchymal Transition. Journal of Biological Chemistry **2011**;286(5):3915-24 doi 10.1074/jbc.M110.162511.
14. Zhang Y, Yan W, Chen X. P63 regulates tubular formation via epithelial-to-mesenchymal transition. Oncogene **2014**;33(12):1548-57 doi 10.1038/onc.2013.101.

15. Onder TT, Gupta PB, Mani SA, Yang J, Lander ES, Weinberg RA. Loss of E-cadherin promotes metastasis via multiple downstream transcriptional pathways. Cancer Research **2008**;68(10):3645-54 doi 10.1158/0008-5472.can-07-2938.
16. Hajra KM, Chen DYS, Fearon ER. The SLUG zinc-finger protein represses E-cadherin in breast cancer. Cancer Research **2002**;62(6):1613-8.
17. Ye Y, Xiao Y, Wang W, Yearsley K, Gao JX, Shetuni B, *et al.* ER alpha signaling through slug regulates E-cadherin and EMT. Oncogene **2010**;29(10):1451-62 doi 10.1038/onc.2009.433.
18. Rodrigues IS, Lavorato-Rocha AM, Maia BdM, Stiepcich MMA, de Carvalho FM, Baiocchi G, *et al.* Epithelial-mesenchymal transition-like events in vulvar cancer and its relation with HPV. British Journal of Cancer **2013**;109(1):184-94 doi 10.1038/bjc.2013.273.
19. Satelli A, Li S. Vimentin in cancer and its potential as a molecular target for cancer therapy. Cellular and Molecular Life Sciences **2011**;68(18):3033-46 doi 10.1007/s00018-011-0735-1.
20. Fincham VJ, Frame MC. The catalytic activity of Src is dispensable for translocation to focal adhesions but controls the turnover of these structures during cell motility. Embo Journal **1998**;17(1):81-92 doi 10.1093/emboj/17.1.81.
21. Bianchi-Smiraglia A, Paesante S, Bakin AV. Integrin beta 5 contributes to the tumorigenic potential of breast cancer cells through the Src-FAK and MEK-ERK signaling pathways. Oncogene **2013**;32(25):3049-58 doi 10.1038/onc.2012.320.
22. Pickard A, Cichon A-C, Barry A, Kieran D, Patel D, Hamilton P, *et al.* Inactivation of Rb in stromal fibroblasts promotes epithelial cell invasion. EMBO J **2012**;31(14):3092-103 doi 10.1038/emboj.2012.153.
23. Lowenstein PR, Enquist LW. Protocols for Gene Transfer in Neuroscience: Towards Gene Therapy of Neurological Disorders. Chichester, NY: Wiley and Sons.; 1996.
24. Mittal MK, Singh K, Misra S, Chaudhuri G. SLUG-induced Elevation of D1 Cyclin in Breast Cancer Cells through the Inhibition of Its Ubiquitination. Journal of Biological Chemistry **2011**;286(1):469-79 doi 10.1074/jbc.M110.164384.
25. Rahman M, Jackson LK, Johnson WE, Li DY, Bild AH, Piccolo SR. Alternative preprocessing of RNA-Sequencing data in The Cancer Genome Atlas leads to improved analysis results. Bioinformatics **2015**;31(22):3666-72 doi 10.1093/bioinformatics/btv377.
26. Heagerty PJ, Lumley T, Pepe MS. Time-dependent ROC curves for censored survival data and a diagnostic marker. Biometrics **2000**;56(2):337-44 doi 10.1111/j.0006-341X.2000.00337.x.
27. Langmead B, Salzberg SL. Fast gapped-read alignment with Bowtie 2. Nature Methods **2012**;9(4):357-U54 doi 10.1038/nmeth.1923.
28. Zhang Y, Liu T, Meyer CA, Eeckhoute J, Johnson DS, Bernstein BE, *et al.* Model-based Analysis of ChIP-Seq (MACS). Genome Biology **2008**;9(9) doi 10.1186/gb-2008-9-9-r137.
29. Myers RM, Stamatoyannopoulos J, Snyder M, Dunham I, Hardison RC, Bernstein BE, *et al.* A User's Guide to the Encyclopedia of DNA Elements (ENCODE). Plos Biology **2011**;9(4) doi 10.1371/journal.pbio.1001046.

30. Liu T, Ortiz JA, Taing L, Meyer CA, Lee B, Zhang Y, *et al.* Cistrome: an integrative platform for transcriptional regulation studies. Genome Biology **2011**;12(8) doi 10.1186/gb-2011-12-8-r83.
31. Mistry DS, Chen Y, Wang Y, Zhang K, Sen GL. SNAI2 Controls the Undifferentiated State of Human Epidermal Progenitor Cells. Stem Cells **2014**;32(12):3209-18 doi 10.1002/stem.1809.
32. Cichon A-C, Pickard A, McDade SS, Sharpe DJ, Moran M, James JA, *et al.* AKT in stromal fibroblasts controls invasion of epithelial cells. Oncotarget **2013**;4(7):1103-16.
33. Gu X, Coates PJ, Boldrup L, Nylander K. p63 contributes to cell invasion and migration in squamous cell carcinoma of the head and neck. Cancer Letters **2008**;263(1):26-34 doi 10.1016/j.canlet.2007.12.011.
34. Candi E, Rufini A, Terrinoni A, Dinsdale D, Ranalli M, Paradisi A, *et al.* Differential roles of p63 isoforms in epidermal development: selective genetic complementation in p63 null mice. Cell Death and Differentiation **2006**;13(6):1037-47 doi 10.1038/sj.cdd.4401926.
35. Boldrup L, Coates PJ, Gu XL, Nylander K. Delta Np63 isoforms differentially regulate gene expression in squamous cell carcinoma: identification of Cox-2 as a novel p63 target. Journal of Pathology **2009**;218(4):428-36 doi 10.1002/path.2560.
36. McKenna DJ, McDade SS, Patel D, McCance DJ. MicroRNA 203 Expression in Keratinocytes Is Dependent on Regulation of p53 Levels by E6. Journal of Virology **2010**;84(20):10644-52 doi 10.1128/jvi.00703-10.
37. Puram SV, Tirosh I, Parikh AS, Patel AP, Yizhak K, Gillespie S, *et al.* Single-Cell Transcriptomic Analysis of Primary and Metastatic Tumor Ecosystems in Head and Neck Cancer. Cell **2017**;171(7):1611-+ doi 10.1016/j.cell.2017.10.044.
38. Wang C, Liu XQ, Huang HZ, Ma HB, Cai WX, Hou JS, *et al.* Deregulation of Snai2 is associated with metastasis and poor prognosis in tongue squamous cell carcinoma. International Journal of Cancer **2012**;130(10):2249-58 doi 10.1002/ijc.26226.
39. Zhao TT, He QT, Liu ZH, Ding XQ, Zhou XF, Wang AX. Angiotensin II type 2 receptor-interacting protein 3a suppresses proliferation, migration and invasion in tongue squamous cell carcinoma via the extracellular signal-regulated kinase-Snai2 pathway. Oncology Letters **2016**;11(1):340-4 doi 10.3892/ol.2015.3898.
40. Jiang FF, Zhou LJ, Wei CB, Zhao W, Yu DS. Slug inhibition increases radiosensitivity of oral squamous cell carcinoma cells by upregulating PUMA. International Journal of Oncology **2016**;49(2):709-19 doi 10.3892/ijo.2016.3570.
41. Chung MK, Jung YH, Lee JK, Cho SY, Murillo-Sauca O, Uppaluri R, *et al.* CD271 Confers an Invasive and Metastatic Phenotype of Head and Neck Squamous Cell Carcinoma through the Upregulation of Slug. Clinical Cancer Research **2018**;24(3):674-83 doi 10.1158/1078-0432.ccr-17-0866.
42. Savagner P, Kusewitt DF, Carver EA, Magnino F, Choi C, Gridley T, *et al.* Developmental transcription factor slug is required for effective re-epithelialization by adult keratinocytes. Journal of Cellular Physiology **2005**;202(3):858-66 doi 10.1002/jcp.20188.
43. Hudson LG, Newkirk KM, Chandler HL, Choi C, Fossey SL, Parent AE, *et al.* Cutaneous wound reepithelialization is compromised in mice lacking

functional Slug (Snai2). Journal of Dermatological Science **2009**;56(1):19-26 doi 10.1016/j.jdermsci.2009.06.009.

44. Dang TT, Westcott JM, Maine EA, Kanchwala M, Xing C, Pearson GW. Delta Np63 alpha induces the expression of FAT2 and Slug to promote tumor invasion. Oncotarget **2016**;7(19):28592-611 doi 10.18632/oncotarget.8696.
45. Serber Z, Lai HC, Yang A, Ou HD, Sigal MS, Kelly AE, *et al.* A C-terminal inhibitory domain controls the activity of p63 by an intramolecular mechanism. Molecular and Cellular Biology **2002**;22(24):8601-11 doi 10.1128/mcb.22.24.8601-8601.2002.
46. Okada Y, Osada M, Kurata S, Sato S, Aisaki K, Kageyama Y, *et al.* p53 gene family p51 (p63)-encoded, secondary transactivator p51 B(TAp63 alpha) occurs without forming an immunoprecipitable complex with MDM2, but responds to genotoxic stress by accumulation. Experimental Cell Research **2002**;276(2):194-200 doi 10.1006/excr.2002.5535.
47. Stabile LP, He GQ, Lui VWY, Henry C, Gubish CT, Joyce S, *et al.* c-Src Activation Mediates Erlotinib Resistance in Head and Neck Cancer by Stimulating c-Met. Clinical Cancer Research **2013**;19(2):380-92 doi 10.1158/1078-0432.ccr-12-1555.
48. Egloff AM, Grandis JR. Targeting epidermal growth factor receptor and Src pathways in head and neck cancer. Seminars in Oncology **2008**;35(3):286-97 doi 10.1053/j.seminoncol.2008.03.008.
49. Koppikar P, Choi SH, Egloff AM, Cai Q, Suzuki S, Freilino M, *et al.* Combined inhibition of c-Src and epidermal growth factor receptor abrogates growth and invasion of head and neck squamous cell carcinoma. Clinical Cancer Research **2008**;14(13):4284-91 doi 10.1158/1078-0432.ccr-07-5226.

Titles and legends to figures

Figure 1. **(A)** Comparison of mRNA expression of SNAI1, SNAI2 and TWIST1 mRNA levels in normal tissue (n=44), human papilloma virus (HPV) +ve (n=36) and HPV-ve (n=241) HNSCC in the TCGA RNA-seq cohort. **(B, C)** Immunofluorescence detection and quantification (Q-score) of Slug protein in normal epithelium and tumour areas from HPV+ve and HPV-ve oropharyngeal HNSCC. N=5 HPV(+ve) and 6 HPV(-ve) tumour sections. **(D)** Fold difference in mRNA expression of TWIST1, SNAI1, SNAI2, VIM and CDH1 genes; and **(E)** protein expression of E-cadherin, Slug, vimentin and β-actin in control (pBabe-HFK) and E6/E7-HFK, respectively. **(F)** Phase contrast images indicating normal cobble stone (green asterix) and elongated spindle-like EMT (red arrows) morphology. **(G)** Immunofluorescence visualisation of E-cadherin (white arrows) and nuclei (DAPI). Scale bars represented as 20μm and 100μm. Data represented as mean±s.e.m. and statistical significance defined as $^{***}P<0.001$, $^{**}P<0.01$, and $^{*}P<0.05$ when calculated by either Welch's t-test (A) or a one-way analysis of variance (C, D) when compared to the normal/controls.

Figure 2. Depletion of Slug expression restores normal phenotype and attenuates cell invasion. **(A)** Fold difference in mRNA expression of SNAI2, VIM and CDH1 genes in Scram siRNA (control) and Slug siRNA mol-1 and mol-2 transfected cells; **(B)** phase contrast images indicating EMT (red arrows) and normal (green asterick) morphology and immunofluorescence visualisation of E-cadherin (white arrows), Slug and nuclei (DAPI) in control (scram) and Slug (mol-2) depleted E6/E7-HFK, respectively. **(C)** Protein expressions of Slug, vimentin, E-cadherin, and β-actin in the same cells as (A); **(D)** H&E staining showing invasions (arrows) on the 3D-organotypic rafts established with control and Slug (mol-2) depleted E6/E7-HFK; and

(E) relative number of invasive incidents across these rafts per cm. Scale bars represented as 20μm and 100μm. N=5 independent experiments. Data represented as mean±s.e.m. and statistical significance calculated by Student's *t*-test with $^{*}P<0.05$ compared to the control, $^{**}P<0.01$ compared to the control.

Figure 3. Depletion of Src expression alleviates EMT. **(A)** Fold difference in mRNA levels and/or **(B)** protein expression of Src, Slug, vimentin, E-cadherin and β-actin in Src (siRNA Src 1 and 2) depleted cells; **(C)** Protein expression of Src-pY^{416}, total Src, Slug, vimentin, E-cadherin and β-actin in E6/E7-HFK treated in the absence and presence of specific Src inhibitor (dasatinib;10, 50 nM). **(D)** Immunofluorescence visualisation of Slug (red) and nuclei (DAPI) on rafts established with E6/E7-HFK and treated in the absence and presence of dasatinib (50 nM). Arrows indicate the invasive incidents in vehicle (control) rafts. High SRC expression correlates to poor survival. **(E)** Comparison of mRNA expression of SRC from normal tissue (n=44), human papilloma virus (HPV)+ve (n=36) and HPV-ve (n=241) HNSCC in the TCGA RNA-seq cohort. **(F)** Kaplan-Meier plots of 5-year overall survival receiver operator curve (ROC) outcome based stratification of low and high mRNA levels of SRC in the above mentioned dataset. Scale bars represented as 100μm. N=3 independent experiments. Data represented as mean±s.e.m. and statistical significance defined as $^{***}P<0.001$, $^{**}P<0.01$, and $^{*}P<0.05$ when calculated by either a one-way analysis of variance (A) or Welch's t-test (E) when compared to the control/normals.

Figure 4. TP63 modulates SNAI2 expression. **(A)** Kaplan-Meier plots of 5-year overall survival receiver operator curve (ROC) outcome based stratification of low and high mRNA levels of TP63 in the in the TCGA HNSCC HPV –ve cohort of 241

patients. **(B)** Visualisation of E6/E7 and normal HFK TP63 ChIP-seq tracks around *SRC* and *SNAI2* loci annotated with Encode histone modification data from normal human epidermal keratinocytes (NHEK) (Myers *et al*, 2011). **(C, D)** Relative mRNA and protein expressions of TP63 and SNAI2 after transient knockdown of total TP63 in E6/E7-HFK. Cells transfected with scram siRNA molecule were treated as the control. N=3 independent experiments. Data represented as mean±s.e.m. and statistical significance calculated by Student's *t*-test with $^{*}P<0.05$ and $^{**}P<0.01$ compared to the controls.

Figure 5. Depetion of different isoforms of TP63 attenuates EMT. **(A)** H&E staining showing invasive incidents (arrows) on 3D-organotypic rafts established with E6/E7-HFK with transient TP63 knockdown by UTR (TP63α, β) and Pan (total TP63) siRNA molecules; and **(B)** quantification of the number of invasive incidents across the rafts per cm established with these cells. **(C, D)** Relative mRNA expressions of TP63α, β, γ isoforms, SNAI2 and SRC; and **(E)** protein expressions of total p63, total Src, Src-pY^{416}, Slug, E-cadherin, vimentin and β-actin after transient knockdown with control (Scram), UTR p63 and Pan p63 molecules in E6/E7-HFK. Scale bars represented as 100μm. N=3 independent experiments. Data represented as mean±s.e.m. and statistical significance calculated by One-way analysis of variance with $^{*}P<0.05$ and $^{**}P<0.01$ compared to the Scram controls.

Figure 6. TP63γ upregulation is sufficient for EMT. **(A)** H&E staining showing invasion (arrows) on 3D-organotypic rafts established after adenovirus-mediated introduction of GFP (control), ΔNp63α, β and γ isoforms in the E6/E7-HFK with stable total TP63 (DBD) depletion; and **(B)** quantification of number of invasive incidents across the rafts per cm established with these cells. **(C)** Relative mRNA levels of TP63γ, SRC, SNAI2 and CDH1 gene; and (**D**) protein expression of HA

(measure of transfected ΔNp63γ), total p63, total Src, Src-pY^{416}, Slug, E-cadherin, vimentin, AKT-pS^{473}, total AKT and β-actin in keratinocytes after adenovirus-mediated expression of GFP and ΔNp63γ isoform. Scale bar represented as 100μm. N=3 independent experiments. Data represented as mean±s.e.m. and statistical significance calculated by One-way analysis of variance and Student's *t*-test with $^{*}P<0.05$, $^{**}P<0.01$ and $^{***}P<0.001$ compared to GFP.

Figure 1

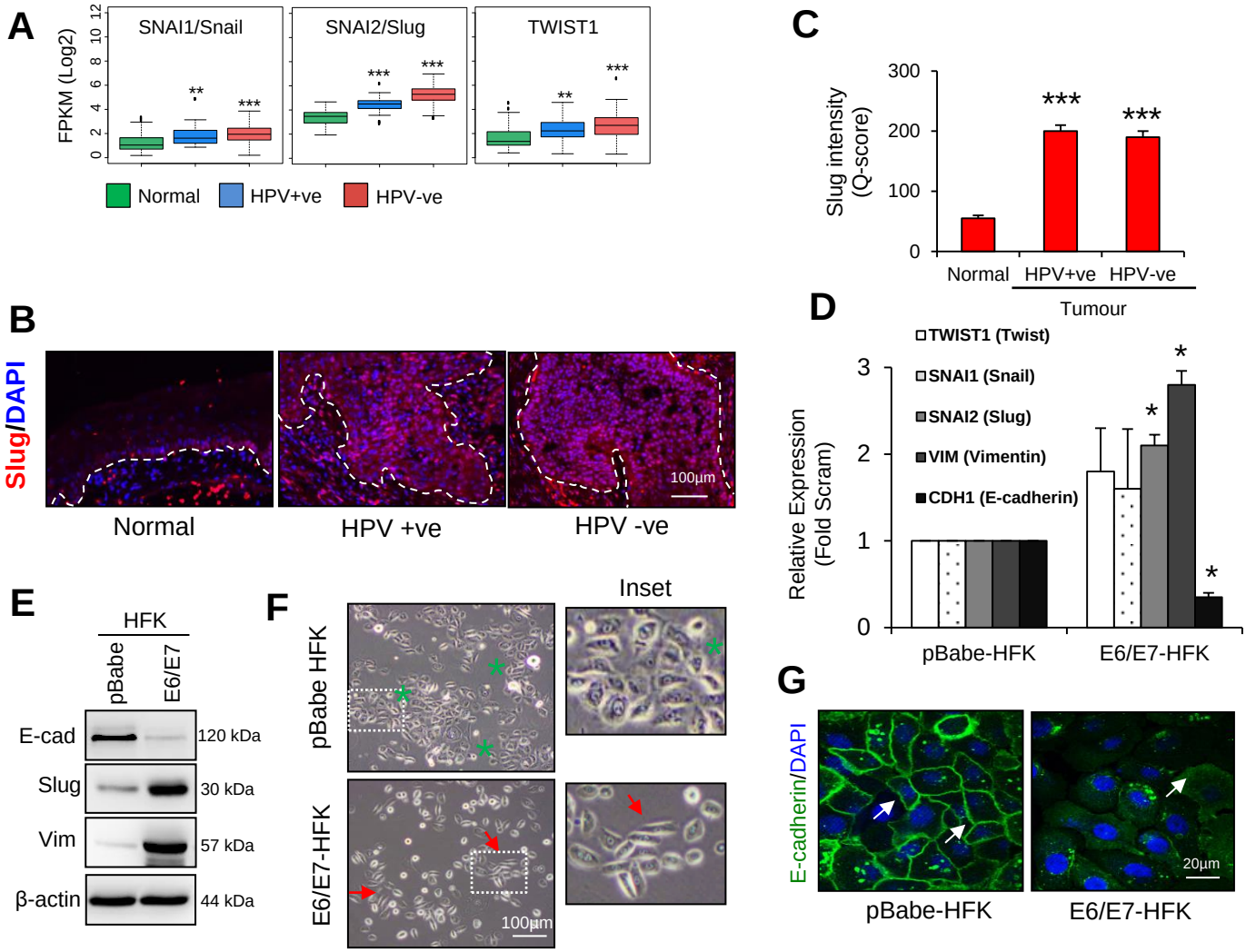

Figure 2

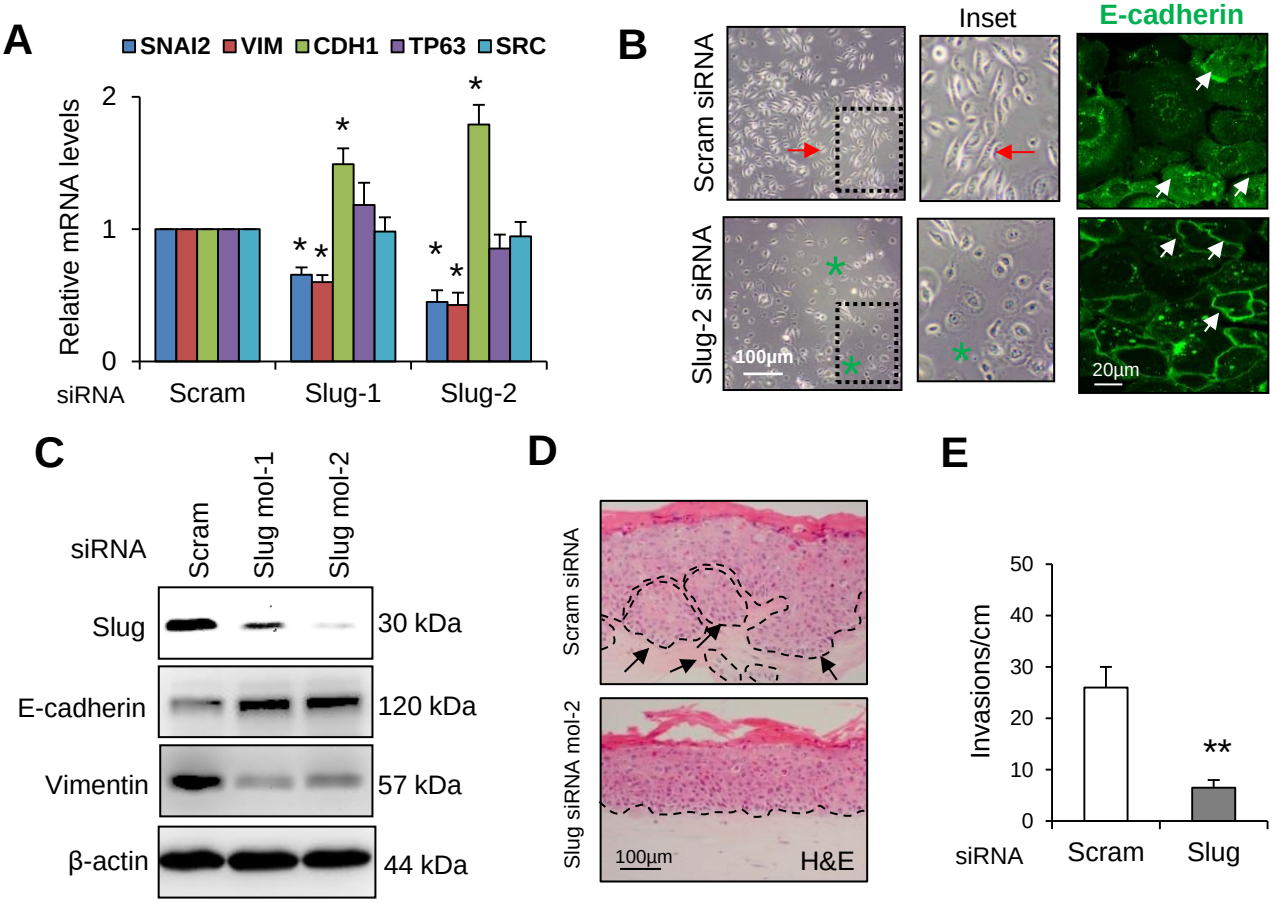

Figure 3

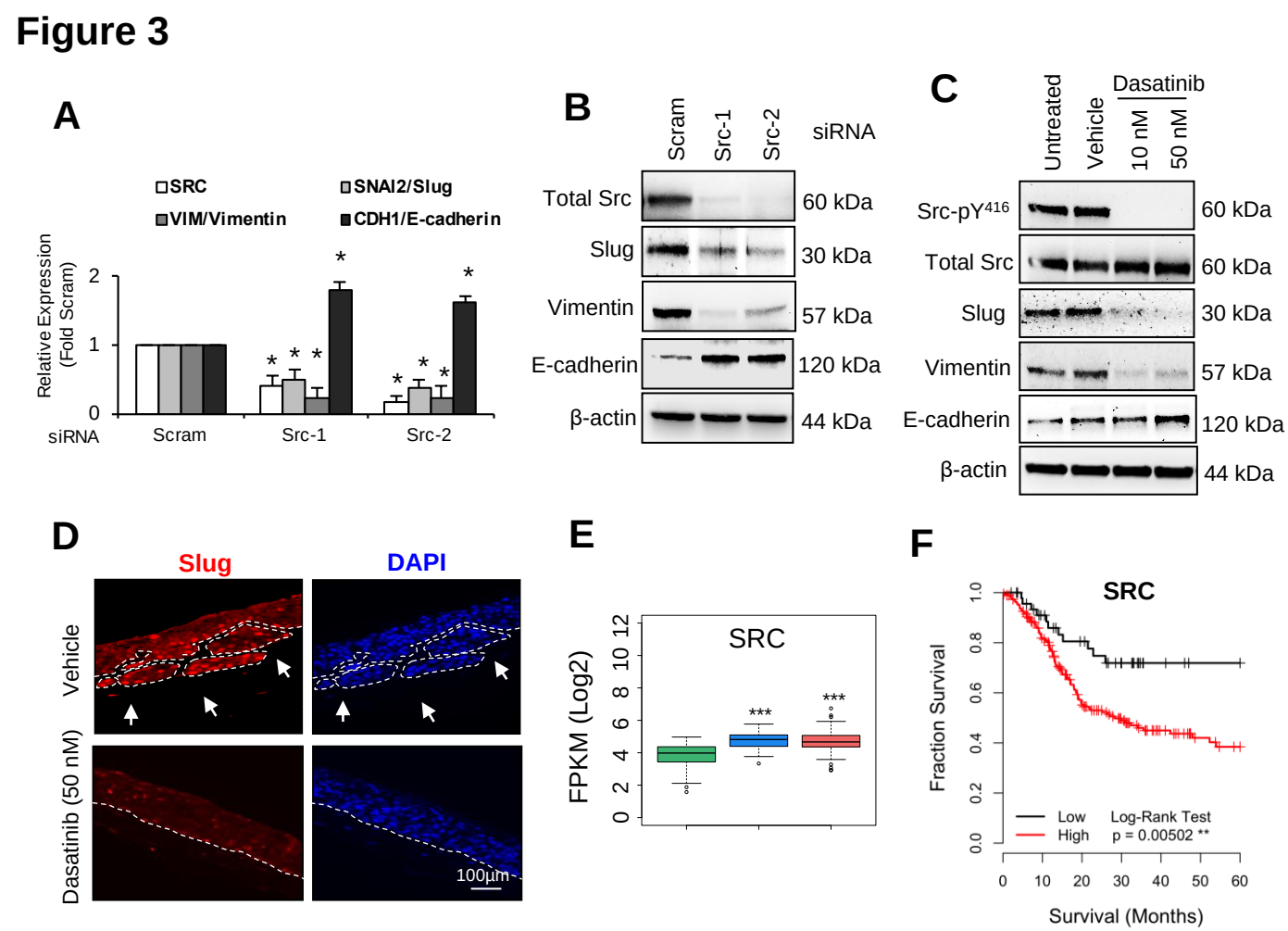

Figure 4

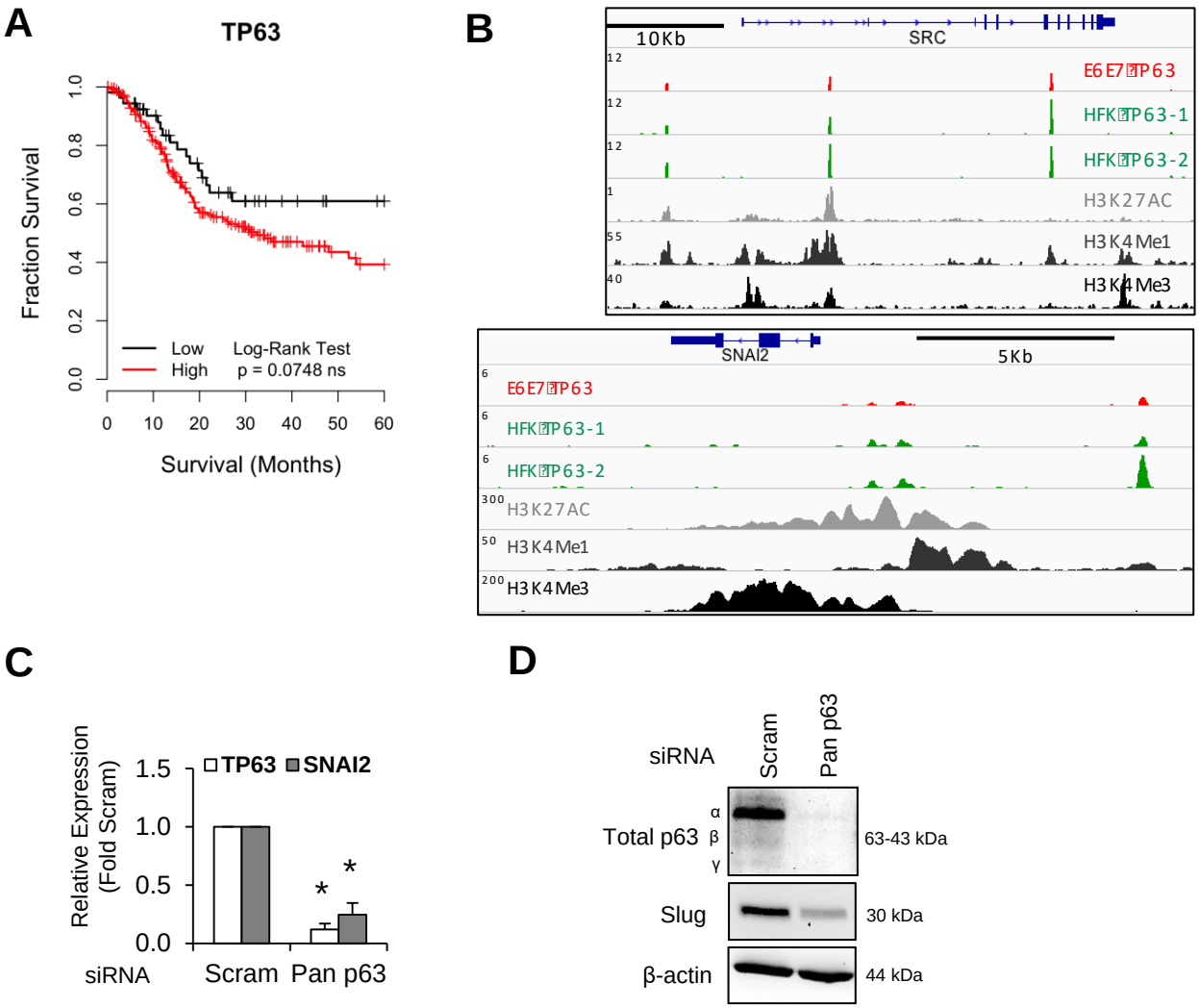

Figure 5

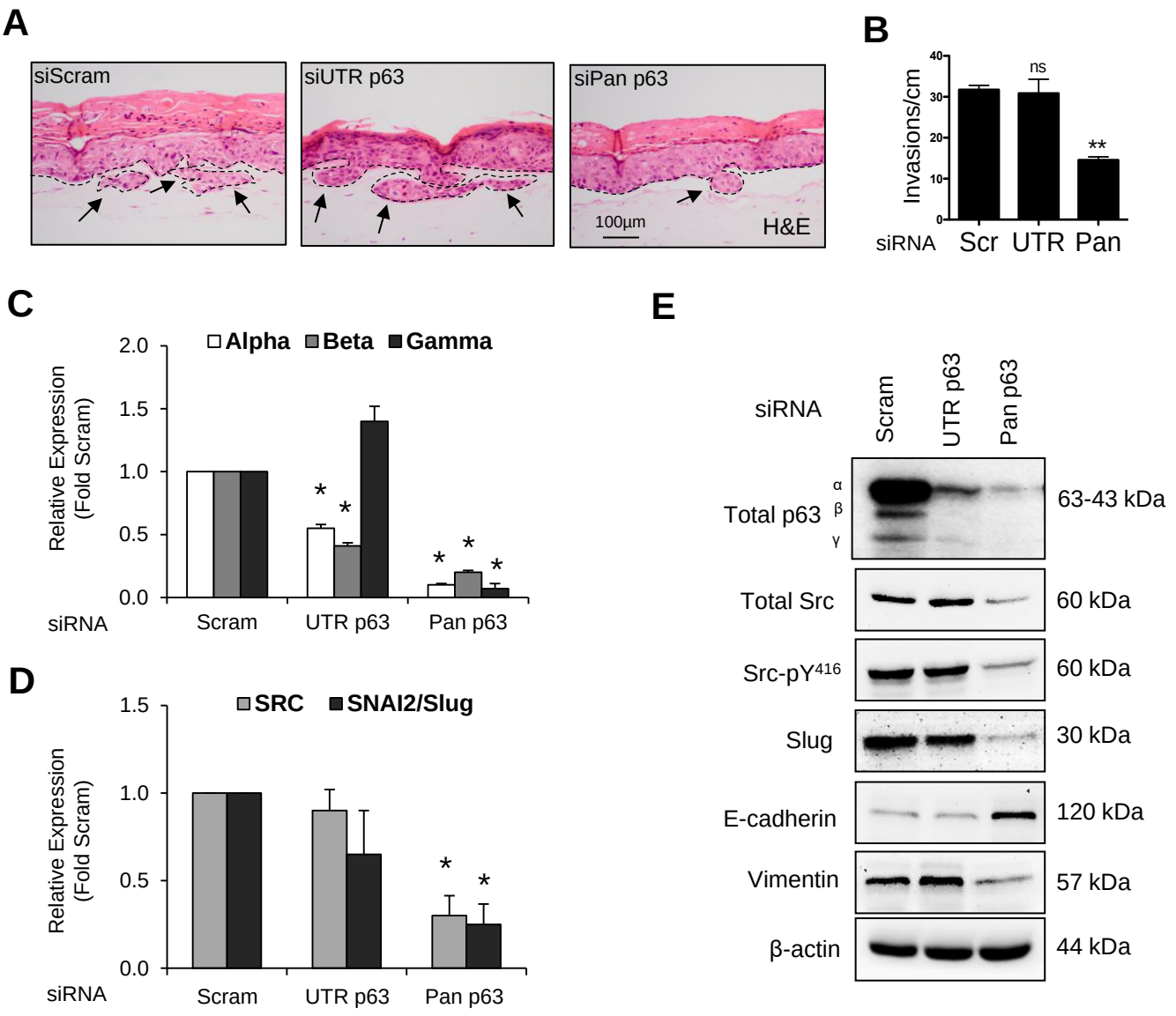

Figure 6

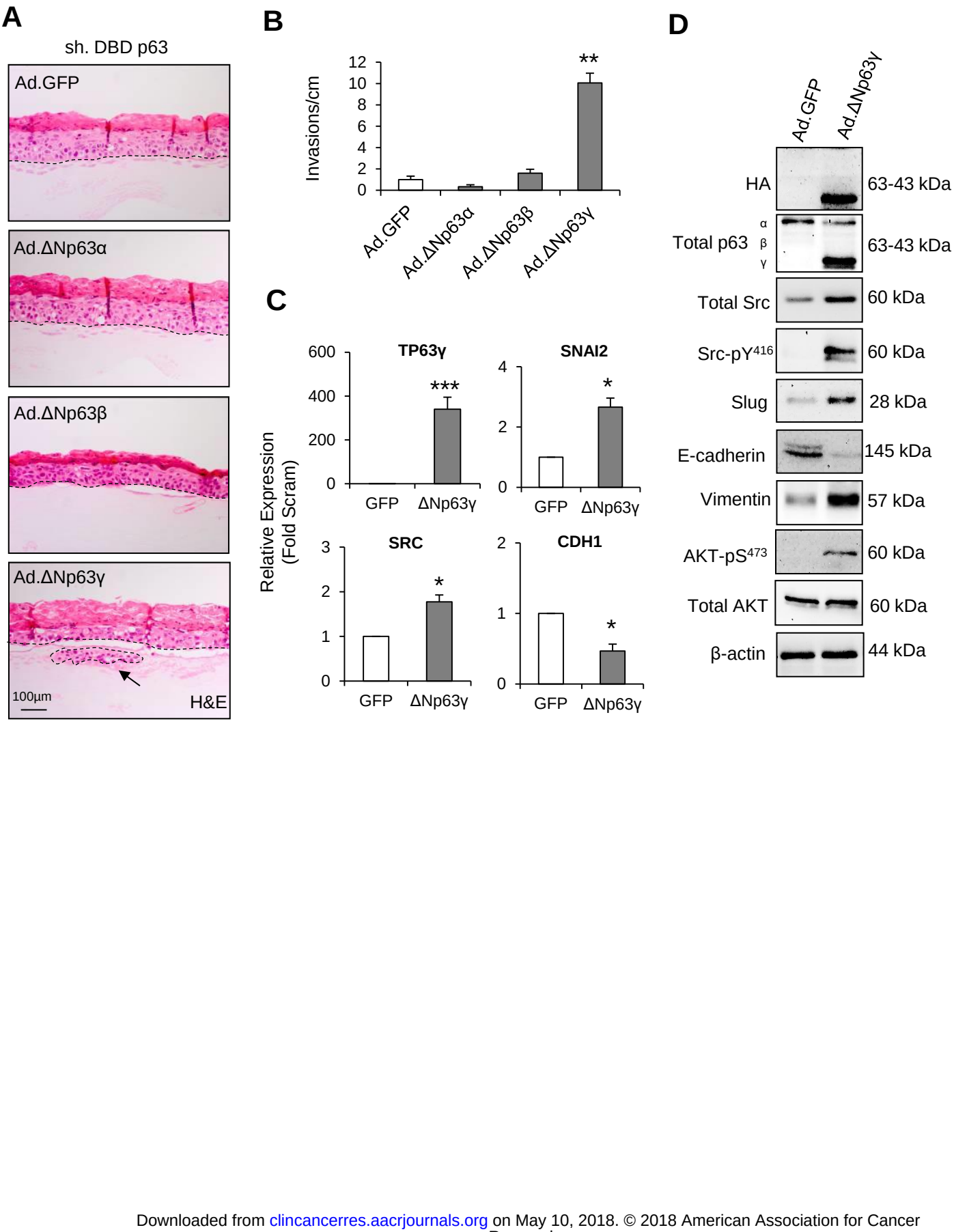

AACR American Association for Cancer Research

Clinical Cancer Research

ΔNp63γ/SRC/Slug signalling axis promotes epithelial-to-mesenchymal transition in squamous cancers

Kirtiman Srivastava, Adam Pickard, Stephanie G Craig, et al.

Clin Cancer Res Published OnlineFirst May 8, 2018.